Journal of Groundwater Science and Engineering
ISSN 2305-7068
Indexed by ESCI CABI CSA
Scopus GeoRef AJ CNKI

Uncertainty analysis of elevation data based on groundwater modeling system: A case study of Zhaozhou County, China

Yun-fei Bai, Zhi-jun Li, Qing Ru, Bo-rui Wang, Jia-jun Li

Citation:
Bai YF, Li ZJ, Ru Q, Wang BR, Li JJ. 2026. Uncertainty analysis of elevation data based on groundwater modeling system: A case study of Zhaozhou County, China. Journal of Groundwater Science and Engineering, 14(4): 582-600.

View online: https://doi.org/10.26599/JGSE.2026.9280096

Articles you may be interested in

Effects of coal mining and tunnel excavation on groundwater flow system in karst areas by modeling: A case study in Zhongliang Mountain, Chongqing, Southwest China
Journal of Groundwater Science and Engineering. 2023, 11(4): 391-407 https://doi.org/10.26599/JGSE.2023.9280031

Karst distribution characteristics in a watershed under topographic differentiation and implication for groundwater resource: A case study in Southwest China using ERT and borehole data
Journal of Groundwater Science and Engineering. 2026, 14(3): 271-287 https://doi.org/10.26599/JGSE.2026.9280083

Developing three-dimensional groundwater flow modeling for the Erbil Basin using Groundwater Modeling System (GMS)
Journal of Groundwater Science and Engineering. 2024, 12(2): 178-189 https://doi.org/10.26599/JGSE.2024.9280014

ANN-based prediction model for single-hole water inflow from piedmont to inland plain areas of Hebei Province, North China Plain
Journal of Groundwater Science and Engineering. 2025, 13(4): 434-448 https://doi.org/10.26599/JGSE.2025.9280064

Research on groundwater ecological environment mapping based on ecological service function: A case study of five Central Asian countries and neighboring regions of China
Journal of Groundwater Science and Engineering. 2024, 12(3): 339-346 https://doi.org/10.26599/JGSE.2024.9280025

Application of the DITAPH model coupling human activities and groundwater dynamics for nitrate vulnerability assessment: A case study in Quanzhou, China
Journal of Groundwater Science and Engineering. 2026, 14(1): 32-48 https://doi.org/10.26599/JGSE.2026.9280069

Journal of Groundwater Science and Engineering 14(2026) 582–600

Journal homepage: http://gwse.iheg.org.cn

Research Article

Uncertainty analysis of elevation data based on groundwater modeling system: A case study of Zhaozhou County, China

Yun-fei Bai[1,2], Zhi-jun Li[1,2*], Qing Ru[1,2], Bo-rui Wang[1,2], Jia-jun Li[1,2]

[1] *School of Hydraulic and Electric-Power*, *Heilongjiang University*, *Harbin* 150080, *China*.
[2] *Institute of Groundwater in Cold Regions*, *Heilongjiang University*, *Harbin* 150080, *China*.

Abstract: This study takes Zhaozhou County in the Songnen Plain (a plain area with sparse borehole data) as the study area, and aims to address the issue of elevation data sources' impact on groundwater numerical simulation by comparatively analyzing the application effects of the Shuttle Radar Topography Mission Digital Elevation Model 90M (SRTM DEM 90M) and interpolated elevation derived from 25 actual boreholes and 14 virtual boreholes (synthetic borehole points derived from DEM data and corrected using nearby measured boreholes). The results show that: The elevation of SRTM DEM 90M can reflect regional microtopographic features; borehole interpolation has single-point errors (−5 m to 10 m) and interpolation uncertainty, and the over-smoothed terrain leads to a relative deviation of 40%–50% in unsaturated zone thickness in specific areas, which further results in a maximum reduction of 93% in evaporation (from 93.92 m^3/d to 6.34 m^3/d). Regarding simulation accuracy, the traditional water level dynamic fitting of both models meets the required standards, but the Nash-Sutcliffe Efficiency (NSE) value of water level fitting for the borehole model is negative, while the statistical indicators of the SRTM model meet the standards. This study confirms that: (1) the "parameter combination effect" plays a dominant role in simulation: Simulation results are essentially the integrated product of multi-parameter interaction; (2) in borehole-sparse areas similar to the Songnen Plain, SRTM DEM 90M can replace borehole interpolation.

Keywords: Groundwater; Digital Elevation Model; Borehole interpolation; Simulation accuracy; Parameter combination effect

Received: 22 Sep 2024/ Accepted: 27 Mar 2026/ Published: 10 Oct 2026

Introduction

Groundwater is a critical strategic water resource for agricultural irrigation, industrial production, and domestic water supply in semi-arid regions of northern China, and numerical simulation has become the core technical tool for regional groundwater resource management, dynamic prediction, and sustainable utilization. As a typical semi-arid plain in the core grain-producing area of Northeast China, the Songnen Plain relies heavily on groundwater to maintain regional water security, especially in Zhaozhou County—the study area of this paper—where there are no large rivers or lakes, and groundwater is the only stable water source for social and economic development. For 3D groundwater flow models, the top elevation of the unconfined aquifer is a fundamental structural input parameter: It directly determines the unsaturated zone thickness, aquifer lithology configuration, vertical hydraulic conductivity, and groundwater evaporation intensity, which are the key processes controlling the accuracy of flow field simulation. Therefore, a systematic assessment of the impact of elevation input data uncertainty on model performance is essential to improve the reliability of groundwater numerical simulation, as validated by numerous case studies in semi-arid regions

*Corresponding author: Zhi-jun Li, *E-mail address*: lizhijun78@163.com

DOI: 10.26599/JGSE.2026.9280096

Bai YF, Li ZJ, Ru Q, et al. 2026. Uncertainty analysis of elevation data based on groundwater modeling system: A case study of Zhaozhou County, China. Journal of Groundwater Science and Engineering, 14(4): 582-600.

2305-7068/© 2026 Journal of Groundwater Science and Engineering Editorial Office This is an open access article under the CC BY-NC-ND license (http://creativecommons.org/licenses/by-nc-nd/4.0)

worldwide (Gaaloul, 2008).

With the continuous development of hydrogeological numerical simulation technology, mainstream modeling tools and aquifer top elevation construction methods for 3D groundwater models have been well established and widely applied. The MODFLOW program has been widely recognized by the global hydrogeological community as one of the most robust and standardized tools for groundwater flow simulation and prediction, due to its clear modular structure, stable numerical solution, and scalable functional modules (Harbaugh, 2005; Langevin et al., 2022; Niswonger et al., 2014; Panday et al., 2013). In recent years, the MODFLOW module embedded in the Groundwater Modeling System (GMS) has become the preferred platform for regional groundwater modeling, thanks to its user-friendly visual operation, efficient pre- and post-processing capabilities, and complete interpolation algorithm library (Chepkemoi et al., 2023). Currently, two mainstream methods are widely used to construct the top elevation of 3D hydrogeological models: the first is the traditional borehole-based interpolation method, which generates the top surface by establishing a Triangulated Irregular Network (TIN) or geostatistical interpolation from measured borehole elevation data (Borgia et al., 2011; Chen et al., 2022; Li et al., 2024); the second is the Digital Elevation Model (DEM)-based method, which uses open-access DEM data (such as the Shuttle Radar Topography Mission (SRTM) DEM 90M) to generate the model top surface through interpolation, which is increasingly used in regional-scale modeling with sparse borehole data (Cromwell et al., 2022; Woolfenden et al., 2022; Zangeneh et al., 2023). Meanwhile, numerous studies have focused on the uncertainty of groundwater numerical models, confirming that input data, boundary condition generalization, and stratum simplification can introduce non-negligible uncertainty to simulation results (Enemark et al., 2024). Scholars have also proposed multi-source data fusion, stochastic simulation, and other methods to quantify and reduce these uncertainties, emphasizing that optimizing the modeling workflow with existing technology is as critical as studying groundwater dynamic distribution (Wellmann and Caumon, 2018; Høyer et al., 2015; Lyazidi et al., 2020).

Despite the above advances, there remain certain limitations in existing research regarding the systematic assessment of how aquifer top elevation data affect groundwater simulation results, especially in semi-arid plain regions without large surface water bodies. First, most existing studies adopt a single top elevation construction method for modeling, and few have carried out a systematic comparative analysis of models with different top elevation inputs under identical stress conditions in the same study area, making it difficult to systematically clarify the advantages, disadvantages, and applicable scenarios of different elevation data. Second, existing studies mostly focus on the overall water level fitting accuracy of the model, but rarely dissect the chain of influence of elevation data differences through the path of unsaturated zone thickness, groundwater evaporation intensity, unconfined aquifer lithology configuration, hydraulic conductivity, and flow field distribution, and thus fail to reveal the internal hydrological process of elevation data affecting simulation results. Third, for semi-arid plain areas such as the Songnen Plain, where groundwater evaporation is the core discharge term and the hydrological process is extremely sensitive to unsaturated zone thickness, targeted research on the impact of elevation data on model performance is still very scarce, which cannot provide reliable methodological guidance for regional high-precision groundwater modeling.

To address the above limitations of existing research, this study systematically investigates the impact of different aquifer top elevation data on groundwater flow simulation results based on the GMS-MODFLOW platform, taking Zhaozhou County, Daqing City, Heilongjiang Province (in the middle of the Songnen Plain) as the study area. The core objective of this study is to assess the response differences of groundwater flow field simulations to the uncertainty of key model structural characteristics (i.e., different aquifer 3D grid top elevation settings) under identical stress conditions, rather than pursuing the long-term predictive capability of a single model. To this end, two sets of 3D heterogeneous anisotropic transient flow models were constructed: One uses SRTM DEM 90M elevation data as the model top surface, and the other uses the interpolation surface generated by 25 measured boreholes and 14 supplementary virtual boreholes as the top surface, with all other boundary conditions, source-sink terms, and hydrogeological parameters kept completely consistent. The trial-and-error method combined with the measured water level data of observation wells was used to calibrate the models. By comparing the performance of the two models from four dimensions: Raw data error characteristics, water level fitting accuracy, unsaturated zone thickness and evaporation response, and aquifer lithology and hydraulic conductivity configuration, and

quantitatively evaluating model performance using three statistical indicators including Nash-Sutcliffe Efficiency (NSE), Root Mean Square Error (RMSE), and Coefficient of Determination (R^2). This study is expected to provide new methodological references and scientific basis for the construction of high-precision groundwater models in similar semi-arid plain regions.

1 Study area

The study area is located in the southwest of Heilongjiang Province (Fig. 1a), in the middle of the Songnen Plain (Fig. 1b). The administrative district level is at the county level, under the jurisdiction of Daqing City, Heilongjiang Province. The county's administrative area is 2,445 km^2, and the grassland area accounts for a large proportion, the annual temperature difference and the daily temperature difference are relatively large, the annual average precipitation is 452.1 mm, and the precipitation is concentrated from June to September, accounting for about 80% of the annual precipitation.

The landform of Zhaozhou County belongs to an alluvial plain, with the topography sloping gently downward from east to west and from north to south, and the landform morphology is relatively uniform (Fig. 2a). The topographic slope was calculated using Geographic Information Systems (GIS) software based on the SRTM DEM 90M dataset. The results show that the topographic slope across the entire study area ranges from 0° to 2°, corresponding to a typical gentle terrain area. There are no natural rivers distributed in the study area; surface runoff occurs only in the rainy season of wet years when rainfall is abundant, and is restricted by various factors. Surface water resources mainly rely on atmospheric precipitation, with evaporation and slight vertical infiltration as the primary discharge pathways. In terms of geological structure, the area is mainly covered by Cenozoic strata: The Quaternary System is widely distributed throughout the region, while the Tertiary System is primarily located in the southern part. The vertical stratification characteristics of the hydrogeological structure are as follows: the shallow layer is a Quaternary porous phreatic aquifer, with lithology dominated by silty clay and fine sand, featuring a thin thickness, uneven distribution, and weak water-bearing capacity; beneath it lie the Quaternary confined aquifer and Tertiary confined aquifer, with lithology mainly consisting of medium sand, fine sand, and gravelly sand (Fig. 2c). These sand layers are characterized by large thickness, extensive and stable distribution, strong permeability, and high water-bearing capacity.

Groundwater in the study area is mainly recharged by atmospheric precipitation infiltration, flows slowly from northeast to southwest (Fig. 2b), and is discharged through artificial exploitation and lateral runoff. The shallow groundwater level is significantly affected by seasonal precipitation, while the deep groundwater level is mainly regulated by exploitation activities. The regional hydrogeological conditions are relatively clear, which can provide a foundation for the generalization of aquifers and parameter partitioning in subsequent numerical simulations.

2 Hydrogeological model preparation

2.1 Hydrogeological conceptual model

To establish the underground aquifer system in the study area, it is necessary to portray the main

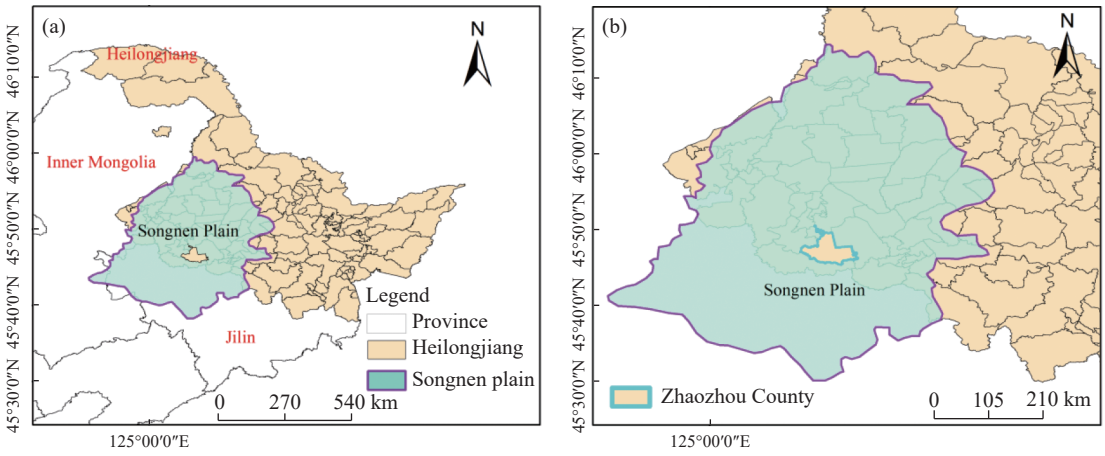


Fig. 1 Geographical map of the study area. (a) geographical location of the Songnen Plain and provincial administrative boundaries; (b) location of Zhaozhou County (the study area) within the Songnen Plain

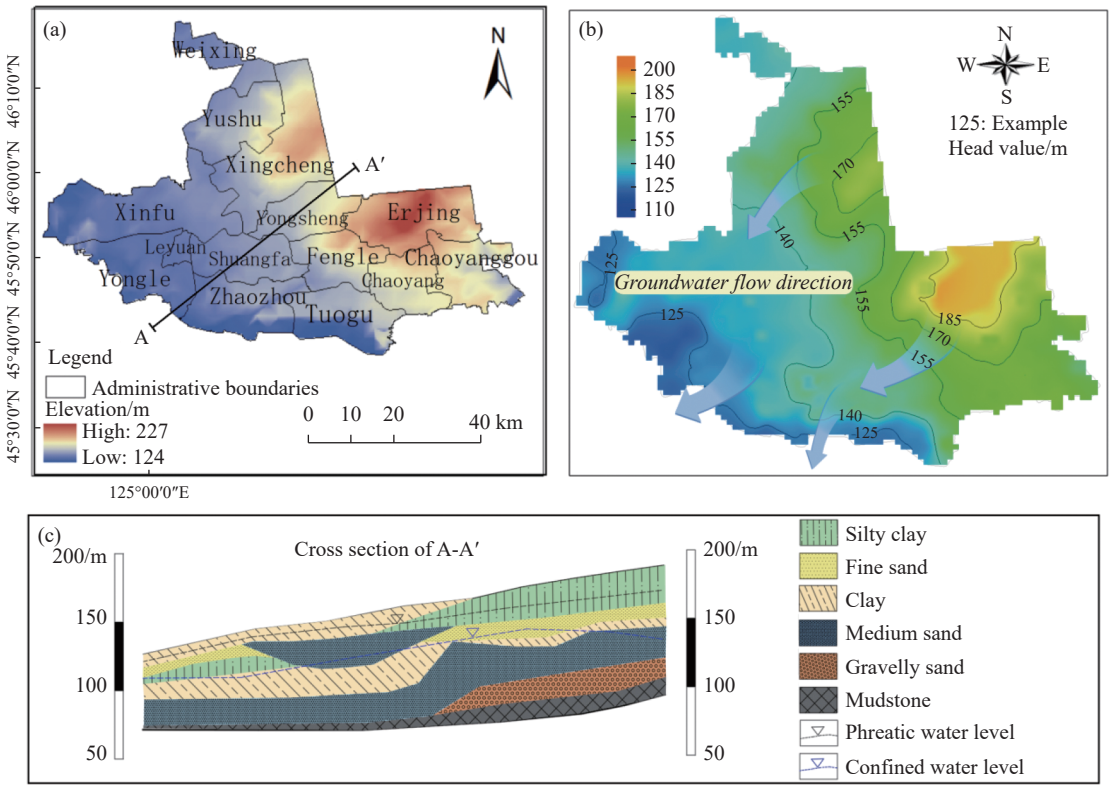


Fig. 2 The information on topographic elevation, township distribution, groundwater flow direction, and A-A' hydrogeological profile of the study area. (a) topographic elevation and township distribution; (b) groundwater flow direction; (c) A-A' hydrogeological profile

factors such as the internal structure of the aquifer, the water exchange situation at the boundary of the study area, and the temporal and spatial distribution of the corresponding parameters in the system. In accordance with the specific hydrogeological conditions, the elements that are weakly related or unrelated to the system should be ignored and simplified appropriately in order to facilitate mathematical expression. The generalization process mainly involves the following aspects: Generalization of the water content properties of the study area, generalization of parameter distributions, generalization of boundary conditions, and generalization of the simulation range of the study area.

This study created a coverage using the administrative boundary of Zhaozhou County, which serves as the natural boundary for all aquifers and defines the spatial scope of the model. According to the analysis of borehole data, the study area aquifer is mainly composed of silt, fine sand, clay, medium sand, and mudstone (Fig. 3). Parameter zoning coverages for the unconfined aquifer, aquitard and confined aquifer were created, and the hydrogeological parameters for different layers

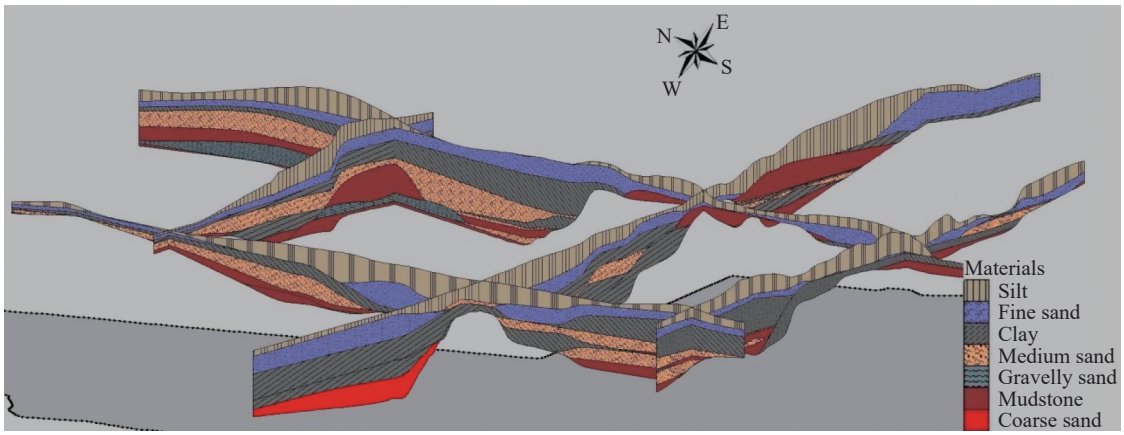


Fig. 3 Three-dimensional geological profile

were comprehensively determined based on the lithology. Subsequently, coverages for source-sink terms and observation points were gradually created. The groundwater type in the study area is pore water. Under the premise of considering the existing technical level, the water exchange in the unsaturated zone of the study area is appropriately neglected and simplified, with the focus on analyzing the impact of changes in lithology and thickness of the unsaturated zone on the water levels of the saturated aquifer. By integrating this information, we generalized the groundwater flow as a three-dimensional transient flow system.

2.2 Generalization of aquifer characteristics

According to the analysis of borehole data, the aquifer medium in the study area is discontinuously distributed in the vertical direction. Due to the alternating changes of the sedimentary environment, it is difficult to find a stable medium for the distribution of the unconfined aquifer, aquitard, and confined aquifer. Maintaining the structural integrity of the aquifer system and adopting a reasonable hydrogeological generalization scheme can effectively improve the reliability of groundwater flow field simulation results (Korus and Joeckel, 2022; Yang et al., 2009). In order to maintain the integrity of the aquifer system and improve the accuracy of groundwater level simulation results, this study generalized silt and fine sand into the unconfined aquifer, and clay as the aquitard between the unconfined and confined aquifers; medium sand and gravelly sand were generalized into the confined aquifer; mudstone was generalized into the watertight boundary (Fig. 4).

Spatially, groundwater flow has horizontal and vertical modes of motion in accordance with conservation of energy and Darcy's law, so groundwater motion can be generalized to three-dimensional flow. The input and output of the groundwater system vary in both time and space, so the groundwater in the study area is unsteady flow. The hydraulic conductivity is not exactly equal in the same direction at each point, and it also varies spatially, reflecting the heterogeneity of the system. The hydraulic conductivity changes with direction, reflecting anisotropy. Therefore, the aquifer can be generalized as non-homogeneous and anisotropic. Based on the known hydrogeological data of the study area and the analysis of the dynamic changes of groundwater in the study area, the aquifer in the study area is generalized as a three-dimensional, non-homogeneous, anisotropic, and transient groundwater flow system.

Due to the continuous distribution of the generalized aquitard in the study area, the hydraulic connection between the unconfined aquifer and the confined aquifer is significantly weakened, so only the unconfined aquifer is simulated in the later MODFLOW.

2.3 Generalization of boundary conditions

Lateral boundary generalization: Groundwater in the study area generally flows from northeast to southwest. Based on the hydrogeological conditions of the study area, the northeastern boundary (AB) is set as the inflow boundary (positive speci-

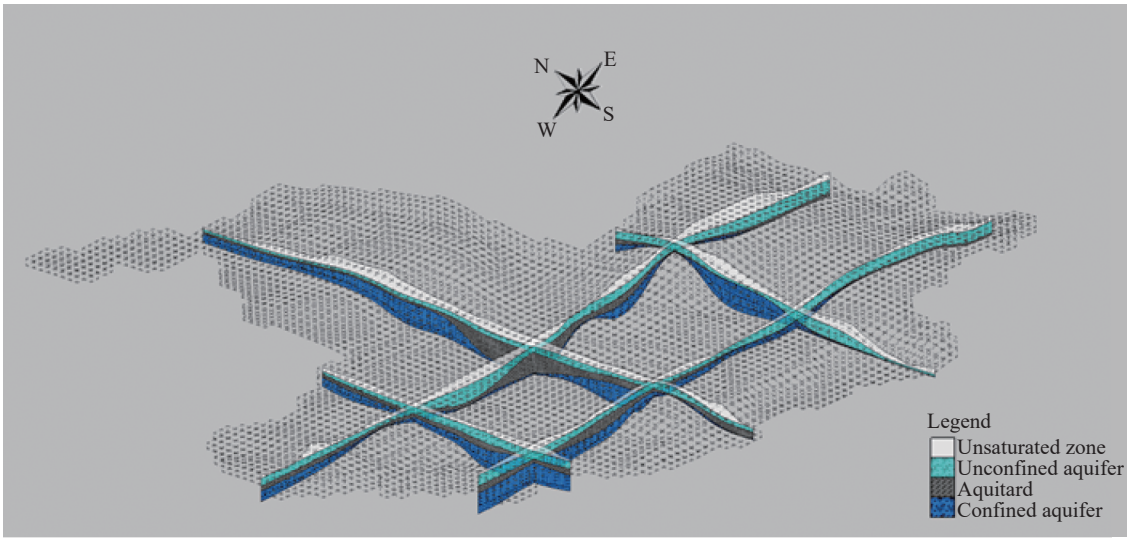


Fig. 4 Aquifer system profile

fied flow), and the southwestern (CD) and southern (EF) boundaries are set as the outflow boundary (negative specified flow), which is realized in MODFLOW using the Well Package (WEL) to assign specified flow rates, collectively referred to as specified flow boundaries (Fig. 5). The flow is determined based on the hydraulic conductivity (K), thickness (M), and hydraulic gradient (I) (Qiu et al., 2015). Other areas have no obvious water exchange and can be generalized as no-flow boundaries. There are no rivers or lakes in the study area, so there are no head-dependent boundaries.

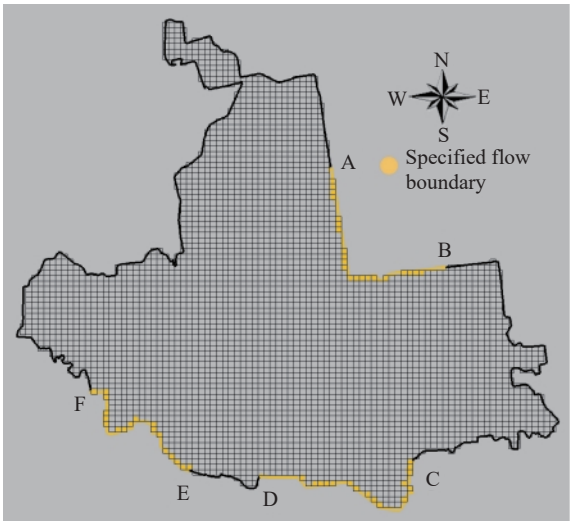


Fig. 5 Boundary conditions of the study area

Vertical boundary generalization: The upper boundary of the study area's groundwater system is the free surface of the unconfined aquifer, and the main water exchange occurs through this phreatic surface with the external system, such as evaporation discharge and atmospheric precipitation infiltration. The bottom layer of the deep aquifer is treated as a no-flow boundary.

3 Groundwater Numerical Simulation Methods

In traditional groundwater numerical modeling, dividing observation data into a calibration period and a validation period is a conventional practice, aiming to verify the effectiveness of calibrated model parameters under different stress conditions (Konikow and Bredehoeft, 1992) and the model's predictive capability. However, the core objective of this study is to assess the impact of uncertainty in key model structural characteristics on groundwater flow field simulations, focusing on comparing the response differences of models with different 3D grid top elevation settings under the same stress conditions rather than pursuing the long-term predictive capability of a single model. Notably, groundwater models are essentially embodiments of scientific hypotheses and cannot be truly "validated"; a good fit during the validation period may stem from the mutual compensation of conceptual errors and parameter uncertainties (Konikow and Bredehoeft, 1992). Beven (1989) pointed out that validation relying on calibrated initial conditions is not truly valid, and parameter interactions can result in multiple parameter combinations that fit the data, making it difficult to reflect the impact of model structure on internal responses. Moreover, parameter simplification in traditional validation is prone to introducing "structural noise", which interferes with the identification of the impact mechanism of target variables (Hunt et al., 2007). Therefore, this study omits the validation period, and only presents and discusses the fitting results and statistical indicators of the calibration period, and focus on analyzing the impact of changes in 3D grid top elevation on model fitting performance, ensuring that the research logic is highly aligned with the core objective.

In this study, two types of elevation data were used: DEM elevation data and elevations from all wellhead and virtual boreholes. The surface elevation data was obtained from the SRTM DEM 90M, sourced from the Geospatial Data Cloud (China, http://www.gscloud.cn/). For the second simulation, Kriging interpolation was performed using all available well and observation borehole elevations, as well as virtual borehole elevations inferred from actual measurement data and stratigraphic trends.

3.1 Governing Equations

This study uses MODFLOW implemented in GMS to simulate groundwater flow, and the governing partial differential equation for three-dimensional groundwater flow solved by MODFLOW is (McDonald and Harbaugh, 1988):

$$\frac{\partial}{\partial x}\left(K_{xx}\frac{\partial H}{\partial x}\right)+\frac{\partial}{\partial y}\left(K_{yy}\frac{\partial H}{\partial y}\right)+\frac{\partial}{\partial z}\left(K_{zz}\frac{\partial H}{\partial z}\right)\pm W=S_y\frac{\partial H}{\partial t} \quad (1)$$

Where: K_{xx}, K_{yy} and K_{zz} represent the hydraulic conductivity in the x, y and z directions (m/d); H is the groundwater head (m); t is the time (day); W is the source-sink term (1/d); S_y is specific yield.

3.2 Construction of the three-dimensional groundwater model

In this study, GMS software was used to establish a three-dimensional groundwater model to study the influence of two types of elevation data on the model results. The software is highly integrated with GIS and has excellent visualization capabilities. It can provide sophisticated subsurface characterization tools and improve the accuracy of groundwater modeling (Al-Areedhi, 2019).

3.2.1 Spatial and temporal discretization

Before simulation, the study area needs to be discretized into grids, and the size of the grid discretization has a very important impact on the modeling accuracy (Sahu and Jhariya, 2023). The scope of this simulation covers the entire county of Zhaozhou. The most commonly used 3D grid in GMS is adopted, dividing the study area into 100 rows and 100 columns in the horizontal direction. The cell spacing in the X-axis direction is 1,224.73 m, and the cell spacing in the Y-axis direction is 1,106.85 m. In the vertical direction, the model is discretized into two layers: the upper layer is designated as the unconfined aquifer, and the lower layer serves as the aquitard. The total number of grid cells is 20,000, including 7,386 active cells (Fig. 6).

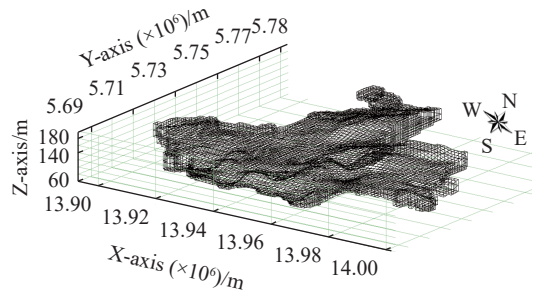


Fig. 6 Three-dimensional odel grid

Based on the available data, 2012, the year with the most comprehensive data, is selected as the calibration period for this simulation. The simulation period is from January 1, 2012, to December 31, 2012, with 12 stress periods defined for the simulation (Baalousha, 2012). Each stress period is subdivided into three time steps. The groundwater levels of 2012 are used as the initial conditions for the model.

3.2.2 Initial value determination

Based on the topography and geomorphology, according to the description of the stratum and aquifer configuration in the survey report and hydrological report, the water-rich distribution pattern of the aquifer, as well as reviewing the relevant numerical modeling literature. The unconfined aquifer composed of multiple media in the study area is divided into 5 geological zones, while the aquitard is not partitioned (Fig. 7).

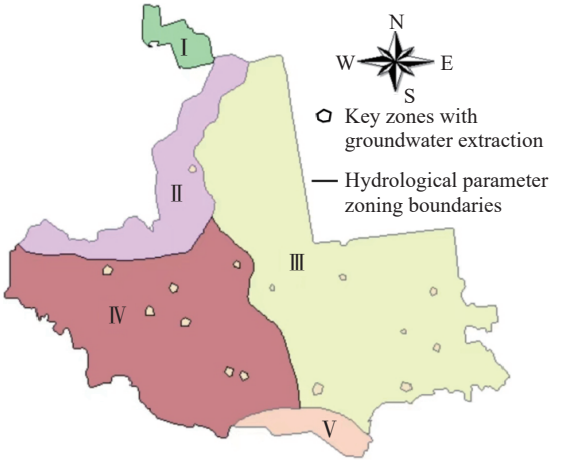


Fig. 7 Hydrological parameters zoning

The key zones with groundwater extraction marked in Fig. 7 correspond to the concentrated multi-well extraction areas for farmland irrigation within the study area, where groundwater dynamics are predominantly controlled by artificial groundwater extraction. The initial hydrological parameters of these zones are assigned consistently with the hydrogeological zones they belong to, and these zones are also predefined as the core areas for source-sink term configuration in the subsequent simulation procedures.

Hydraulic parameters such as horizontal hydraulic conductivity (K_h), vertical hydraulic conductivity (K_v), specific storage (S_s), specific yield (S_y), and effective porosity are defined. Each of the hydraulic parameter values in Table 1 is selected with reference to the comprehensive hydraulic conductivity of lithology after aquifer generalization and previous research results in this region. The final parameter values were determined by the trial estimation-correction method from the subsequent model calibration stage.

3.2.3 Calculation and treatment of source and sink items

Source and sink terms represent the recharge and discharge of the groundwater system. Groundwater recharge includes: Rainfall infiltration; irrigation infiltration, and lateral recharge; while discharge includes phreatic evapotranspiration; groundwater abstraction; and lateral discharge.

When processing irrigation infiltration recharge data, since irrigation primarily occurs on arable land, the 2012 land use map of Zhaozhou County

Table 1 Hydraulic parameters values

Type of aquifer	Parameter partitioning	K_h (m/d)	K_v (m/d)	S_y	S_s (1/m)	Effective porosity
Unconfined aquifer	Ⅰ	4	0.4	0.1		0.3
	Ⅱ-Ⅳ	6	0.6	0.1		0.3
	Ⅴ	8	0.8	0.1		0.3
Aquitard		0.001	0.0001		0.000001	0.3

Notes: The starting head in the model uses the water level data observed in the observation wells on January 1,2012.

is input into ArcGIS, where the arable land area is overlaid with the township-level administrative map. The units are selected for division, and simplified treatment is carried out during the simulation. The irrigation infiltration recharge for the irrigation period from May to August, totaling 123 days, is converted into recharge intensity and merged into the rainfall infiltration recharge. The overlapping areas are calculated using Microsoft Excel. The rainfall infiltration is calculated using the same recharge coefficient, and is simulated using Recharge Package (RCH) (Kawo et al., 2023). The rainfall and evaporation of the study area in 2012 are shown in Table 2.

After organizing the data, the ratio of agricultural irrigation volume to the area of the township is used to estimate the equivalent recharge depth. This value is divided by the irrigation period (123 days) and multiplied by the irrigation infiltration recharge factor to obtain the recharge rate. The agricultural irrigation volume and recharge rate for each township in the study area from May to August 2012 are shown in Table 3.

The lateral recharge is estimated based on hydrological parameters such as K, M, and I, and is approximately 2,263 m^3/d (AB), while the discharge amounts to approximately −1,231 m^3/d (CD) and −347 m^3/d (EF).

According to the relevant project reports and literature of the study area, the extinction depth of evapotranspiration is 4 m. Evapotranspiration is calculated based on data from the Zhaozhou County meteorological station, and a uniform phreatic evaporation coefficient is applied across the region. During the freeze-thaw period, part of the recharge to the groundwater system comes from the melting of water in the frozen soil; however, there are many uncertain factors in the

Table 2 Monthly rainfall and evaporation in 2012

Month	1	2	3	4	5	6	7	8	9	10	11	12
Rainfall (mm)	0.1	1.6	11.6	27.9	11.7	99.9	118.4	48.5	68.6	36.2	31.6	9.8
Evaporation (mm)	11.8	27	91.1	228.3	320.1	270	213.7	177.2	148.2	112.2	43.1	16.5

Table 3 Agricultural irrigation volume

Township	Area (km^2)	Irrigation volume (10^4 m^3)	Recharge rate (m/d)
Shuangfa Township	145.52	151.7	0.000011
Tuogu Township	184.07	166.9	0.0000096
Zhaozhou Town	200.51	390.7	0.0000206
Yongle Town	175.88	185.6	0.0000112
Xinfu Township	358.79	333.1	0.0000098
Xingcheng Town	340.54	287.8	0.0000089
Fengle Town	132.2	174.7	0.000014
Yongsheng Township	136.03	164.7	0.0000128
Yushu Township	184.28	186.5	0.0000107
Chaoyanggou Town	156.05	189.7	0.0000128
Chaoyang Township	131.64	147.8	0.0000119
Erjing Town	230.37	297.7	0.0000137
Weixing Breeding Farm	85.06	60.1	0.0000075
Le Yuan Township	25.26	22.9	0.0000096

calculation of this portion, and therefore it is often not considered.

According to analysis of groundwater extraction intensity in Zhaozhou County, groundwater extraction is divided into point extraction of groundwater under different spatial and temporal distributions, and groundwater extraction during the irrigation period from May to August. The spatial distribution of the aforementioned irrigation groundwater extraction areas is fully consistent with the key zones with groundwater extraction marked in Fig. 7. Then, according to the township's daily extraction volume and intensity zoning, the groundwater extraction volume is distributed to the corresponding grid cells and simulated using the Well Package (WEL) (Kheirandish et al., 2020). The major recharge coefficients for the study area are shown in Table 4.

Table 4 Main coefficients for the study area

Study area/ km^2	Rainfall infiltration recharge factor	Irrigation infiltration recharge factor	Soil evaporation coefficient
2,445	0.189	0.13	0.042

3.2.4 Model calibration

A total of 15 observation wells in the unconfined aquifer were used in the study area, and the IDs of the observation wells were G1, G2, G3, G4, G6, G9, G11, G12, G14, G15, G16, G17, G22, G24, and G25 (Fig. 8), respectively. The observed groundwater level data come from the Zhaozhou County Water Authority (China). The results of the transient model simulation (calculated water levels as of December 31, 2012) are shown in Fig. 8.

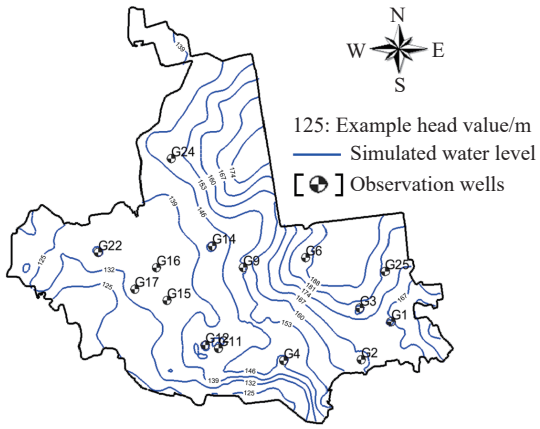


Fig. 8 Distribution of observation wells and simulated water level

The time series of calculated and observed water levels for each observation well are shown in Fig. 9.

In this study, the model's performance was evaluated using statistical indicators such as Nash-Sutcliffe Efficiency (NSE), Root Mean Square Error (RMSE), and Coefficient of Determination (R^2). A value of NSE close to 1 indicates that the model's simulation results are highly consistent with the observed values, while a negative value suggests poor model performance. The Root Mean Squared Error (RMSE) measures the deviation between the model's calculated values and the observed values, with a smaller value indicating better model performance (Gao et al. 2023). The Coefficient of Determination (R^2) is used to assess the model's ability to explain the variability of the data, ranging from 0 to 1, with values closer to 1 indicating that the model can adequately represent for the variability in the data (Zhai et al., 2023). The statistical results for each observed and calculated value are shown in Fig. 10.

The results of the aforementioned statistical indicators demonstrate that the model, after calibration, has reliable parameters that can effectively reflect the hydrogeological conditions of the study area. The calibrated hydrogeological parameters for each zone are presented in Table 5. It should be noted that other hydrogeological parameters were not adjusted, as they were already consistent with the water level simulation results.

During the calibration process, since G1 and G2 could not be fully matched, a local calibration was performed for G1 and G2. The reasons for this may be: (1) Potential inconsistencies in the parameter zoning. (2) G1 and G2 are located in groundwater abstraction areas, where the abstraction rates are not accurately quantified, introducing uncertainty. The results of parameter calibration are shown in Table 6. The local zoning is shown in Fig. 11.

3.3 Construction of virtual boreholes

To address the potential terrain surface interpolation distortion caused by sparse actual borehole data (only 25 in total), this study utilizes the Create Borehole tool in GMS software to construct supplementary virtual boreholes. The construction process adheres to the principle of "actual measurement data dominance", strictly controlling the proportion of virtual data, and defines three standardized steps. It should be noted that wells numbered G5, G7, G8, G10, G13, G18, G19, G20, G21, and G23 are observation wells of the confined aquifer; thus, they were not imported into the model for unconfined aquifer calibration, and

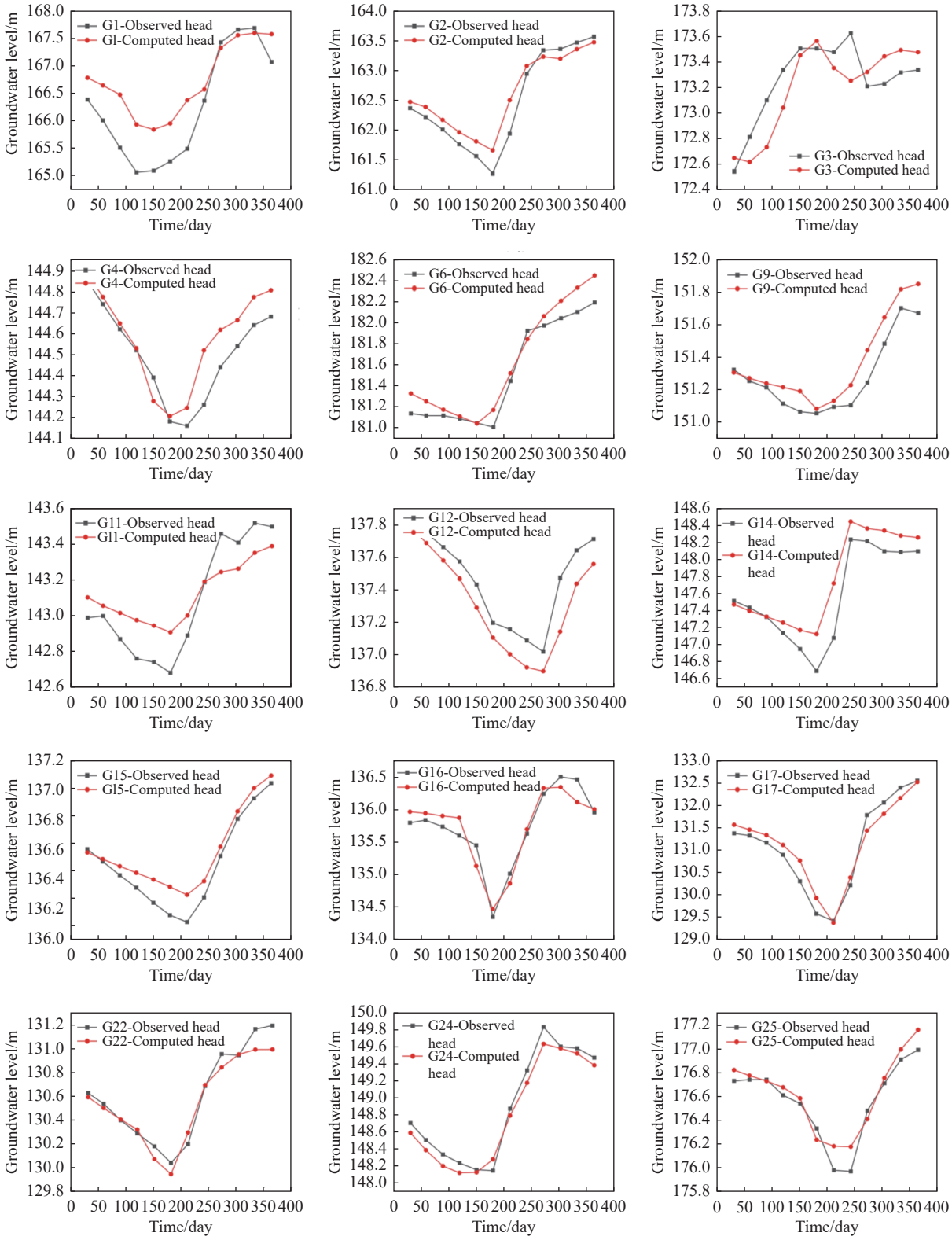


Fig. 9 Comparison chart of computed (red) and observed (black) water levels

only their original elevation attributes were utilized in this study.

3.3.1 Basis for quantity control

Taking 50% of the number of actual boreholes as the baseline while considering the layout requirements of key areas, this study has a total of 25 actual boreholes, thus setting the upper limit of virtual boreholes at 12–13. After comprehensively evaluating the necessity of layout in key areas (see the distribution principles below), the final number of virtual boreholes to be constructed is determined as 14, accounting for 56% of the actual

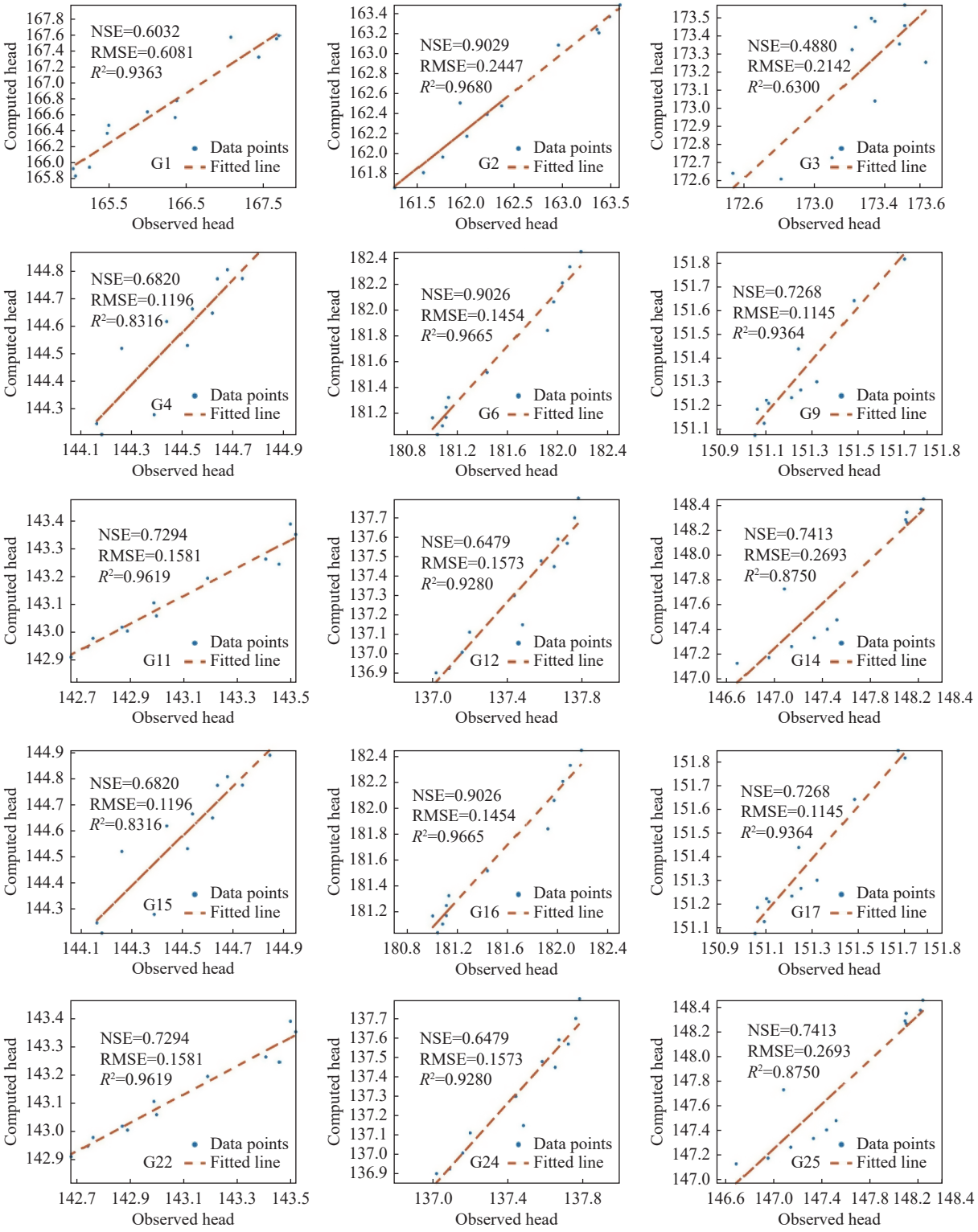


Fig. 10 Scatter Plot with Fit Line

boreholes. This proportion not only effectively supplements spatial information but also ensures that the model takes actual measurement data as the absolute core.

3.3.2 Elevation generation method

The top elevation of each virtual borehole is generated using a two-step correction method to ensure consistency with the regional topographic trend and local measured data:

Reference Value Extraction: Extract the elevation at the coordinates (x, y) of the virtual borehole from the SRTM DEM data, which serves as the reference value Z_{srtm}.

Table 5 Hydrogeological parameter calibration results

Parameter partitioning	Hydraulic conductivity (m/d)	Specific yield
Ⅰ	4.57	0.06
Ⅱ	6.35	0.08
Ⅲ	7.64	0.12
Ⅳ	6.42	0.09
Ⅴ	8.95	0.14

Table 6 Ⅵ and Ⅶ, hydrological parameter calibration results

Parameter partitioning	Hydraulic conductivity (m/d)	Specific yield
Ⅵ	7.94	0.11
Ⅶ	7.89	0.11

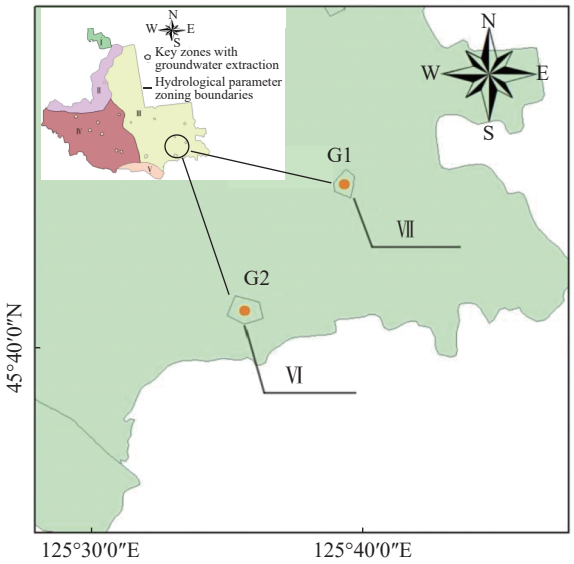


Fig. 11 Local zoning for G1 and G2

Local Correction: Calculate the difference between the SRTM elevation and the measured elevation at the nearest actual borehole to the virtual borehole (i.e., local correction amount ΔZ), and correct the reference value. The calculation formula is as follows:

$$Z_{virtual} = Z_{srtm} - \Delta Z \quad (2)$$

$$\Delta Z = Z_{srtm,nearest} - Z_{obs,nearest} \quad (3)$$

Where: $Z_{virtual}$ refers to the final top elevation of the virtual borehole (m); Z_{srtm} denotes the SRTM elevation at the virtual borehole location (m); $Z_{srtm,nearest}$ and $Z_{obs,nearest}$ refer to the SRTM elevation and the measured top elevation of the nearest actual borehole (m).

3.3.3 Spatial distribution principles

The spatial locations of virtual boreholes are arranged based on the principle of "filling key information gaps" (with their spatial distribution shown in Fig. 12), specifically including three types of regions, as detailed in Table 7.

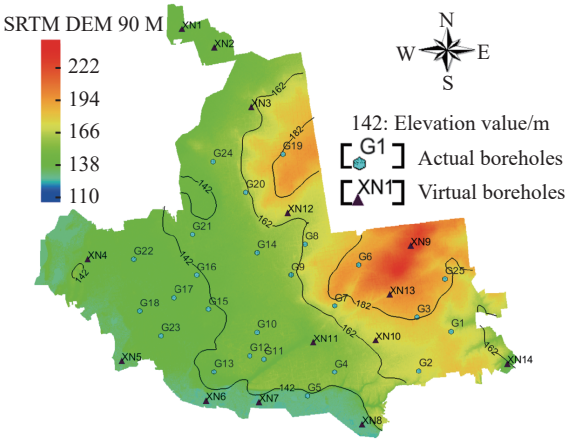


Fig. 12 Distribution of actual and virtual boreholes

4 Comparative analysis and discussion

4.1 Original errors

4.1.1 Error of SRTM DEM 90M

The SRTM DEM 90M data used in this study have been systematically evaluated for their accuracy in the study area (Songnen Plain). According to the research by Zhang et al., (2018), the elevation deviation between the SRTM DEM 90M and topographic data in the Songnen Plain (Fig. 2a) is mainly distributed within the range of −2 m to 2 m.

4.1.2 Error of borehole data

The interpolated terrain surface generated based on

Table 7 Basis for the layout of virtual boreholes

Type	Virtual borehole numbering
Information gap areas	XN1, XN2, XN3, XN4, XN11
Areas with high topographic gradient (areas with distinct color transitions in Fig. 12)	XN9, XN10, XN12, XN13
Boundary areas of the study area	XN5, XN6, XN7, XN8, XN14

39 control points (25 actual boreholes + 14 virtual boreholes) has a fundamentally different error characteristics from the SRTM DEM: Measurement error at specific borehole locations and interpolation error at locations without boreholes.

Measurement Error at Specific Locations: Temporarily remove the value of one known point, use the remaining 38 points for interpolation to predict the value of the removed point, and then calculate the error between the predicted value and the actual value. This method was applied sequentially for all 39 points, and the results show that the single-point error of borehole data ranges from −5 m to 10 m.

Interpolation Error at Locations Without Boreholes: This error is highly uncertain in this study and cannot be quantitatively described. The Kriging interpolation algorithm performs data filling in areas without boreholes, which may generate topographic features that do not actually exist.

4.1.3 Surface Elevation Comparison

The study area boundary shapefile is imported in GMS, the model domain boundary is defined, and the above boreholes are used to automatically assign stratigraphy, The "Horizons to Solid" option is selected, and the borehole elevation is used as the upper boundary to construct the 3D groundwater flow model. Other conditions remain unchanged, and the model comparison after changing only the elevation is shown in Fig. 13.

From Fig. 13, it can be observed that the model established by the borehole elevations (right panel) shows no fine sand exposed on the surface.

4.2 Comparison of simulation results

Without changing the source-sink terms, boundary conditions, stress periods, time steps, etc., the model is rerun using the borehole elevation data for parameter calibration. After parameter calibration, the model simulation results are compared with those obtained using SRTM DEM. The comparison results further reflect the impact of initial elevation errors on the model. As shown in Fig. 14, the results of the parameter calibration are shown in Table 8.

Select observation wells G9 and G22, which have high degrees of water level agreement in the study area, for error comparison (the errors in other areas are relatively greater), and the comparison results are shown in Fig. 15.

Based on the data comparison in Fig. 15, the water level dynamics of the models constructed using the two types of data meet the traditional fitting requirements. However, comparisons of statistical indicators show that while the simulation results using borehole elevation data are to a certain extent representative, the results simulated with SRTM DEM elevation data are more accurate with relatively smaller errors, and thus superior to those using borehole elevation data.

This difference directly originates from the initial errors of the two elevation datasets: The large single-point and interpolation errors of borehole data are transmitted to the water level simulation, while the stable small deviation of SRTM DEM ensures higher fitting accuracy.

4.3 The influence mechanism of surface elevation on unsaturated zone thickness

The deviation of simulation results is not isolated; it further affects the key hydrogeological characteristics of the unsaturated zone, which is closely related to surface elevation.

The accuracy of surface elevation data directly affects the calculation accuracy of unsaturated zone thickness. The unsaturated zone thickness is determined by the elevation difference between

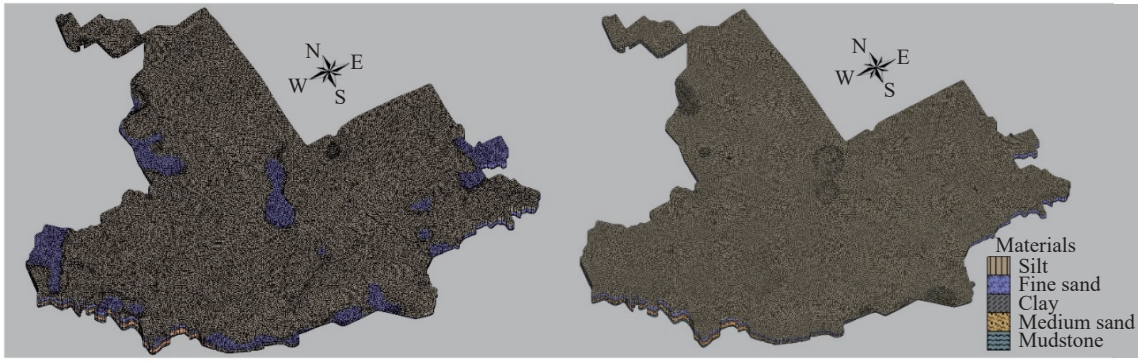


Fig. 13 Surface elevation comparison (left - SRTM DEM, right - Borehole elevation)

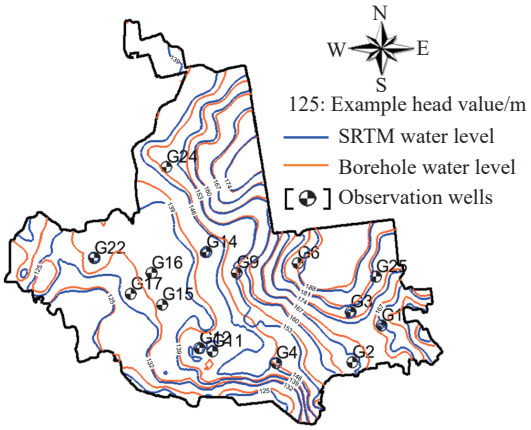


Fig. 14 Comparison of simulation results

Table 8 Hydrogeological parameter data

Parameter partitioning	Hydraulic conductivity (m/d)	Specific yield
Ⅰ	2.46	0.06
Ⅱ	4.88	0.07
Ⅲ	5.45	0.11
Ⅳ	5.31	0.08
Ⅴ	6.87	0.12

ground surface elevation and the groundwater level. By comparing the models constructed using the two elevations datasets (Fig. 16), the following key patterns are identified:

4.3.1 Spatial deviation characteristics

The SRTM DEM model (Fig. 16 left) shows that the spatial distribution of the unsaturated zone thickness is smooth, which is consistent with topographic relief.

The borehole elevation model (Fig. 16 right) shows systematic overestimation in the northeastern and western regions, with a local maximum deviation of 6.0 m.

Points at the same position in typical areas were selected for quantitative analysis. As shown in Table 9. The relative deviation of the unsaturated zone thickness between the borehole model and the SRTM model reaches 40%–50%. This significant deviation is attributed to the over-smoothed surface elevation of the borehole model (Section 4.1.3), which distorts the elevation difference between the ground surface and the groundwater level.

4.3.2 Deviation formation mechanism

Sparse borehole data are insufficient to capture the microtopography identified in the SRTM DEM, resulting in Kriging interpolation generating over-smoothed surfaces (Fig. 13 right). Even with the supplement of virtual boreholes, the terrain surface is still constrained by the limited actual borehole

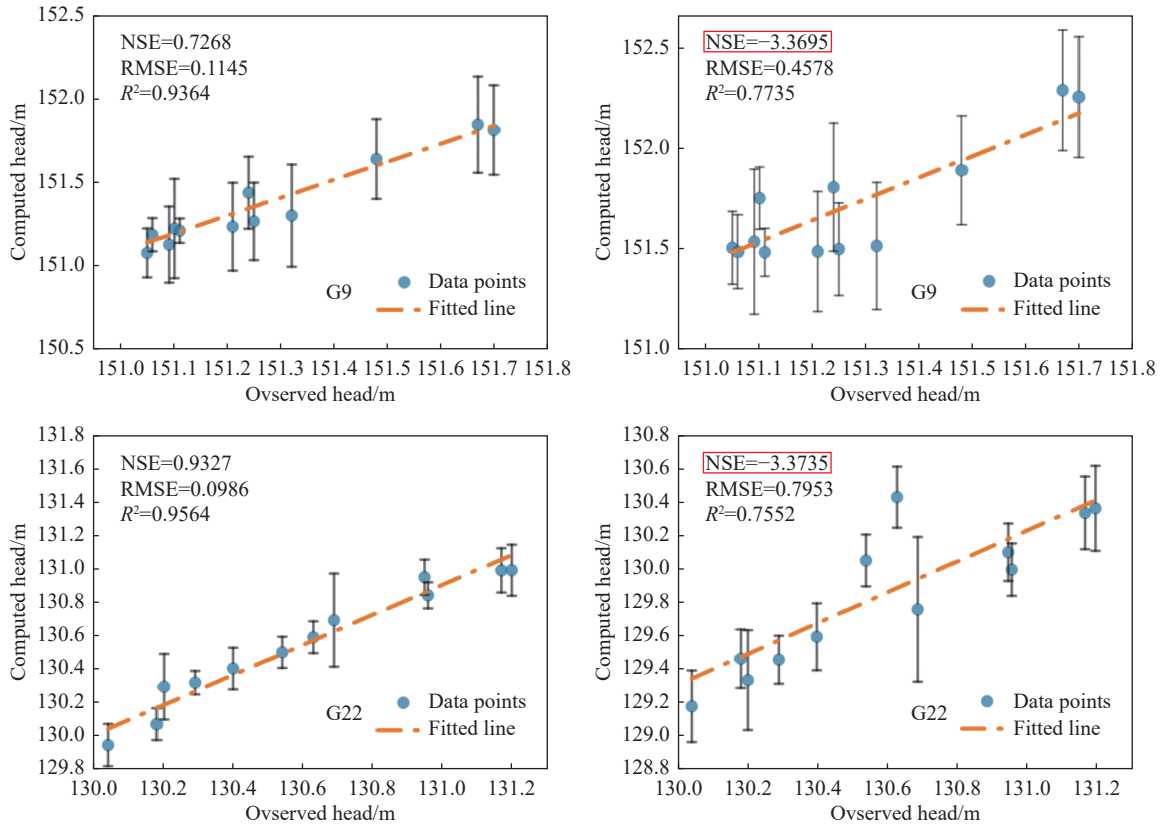


Fig. 15 Statistical indicator comparison chart (left - SRTM DEM, right - Borehole elevation)

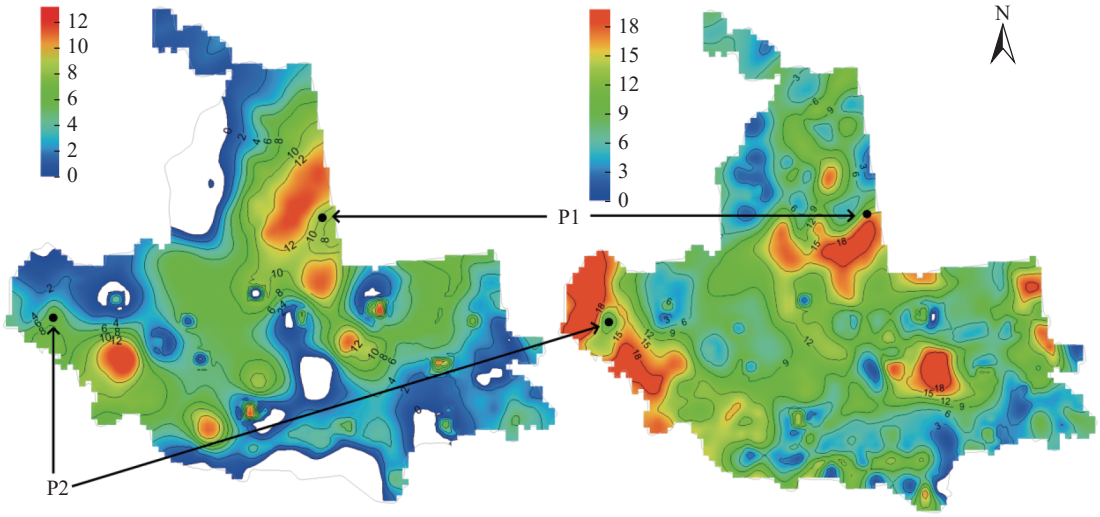


Fig. 16 Comparison of spatial distribution of unsaturated zone thickness (left - SRTM DEM, right - Borehole elevation)

Table 9 Analysis of unsaturated zone thickness

Position	SRTM DEM thickness (m)	Borehole model thickness (m)	Relative deviation (%)
Northeast P1	8.2	12.3	50.0
Western P2	6.5	9.1	40.0

data (25 points), and therefore cannot reproduce the local microtopography reflected by the SRTM DEM. This over-smoothing directly leads to the overestimation of unsaturated zone thickness in the borehole model.

4.3.3 Impact of hydrological processes

The overestimation of unsaturated zone thickness will lead to the underestimation of groundwater evaporation, the extension of rainfall infiltration path, and the enhancement of the recharge lag effect.

To further clarify the relationship between unsaturated zone thickness and evaporation, an experiment was conducted using data from point P2: The entire surface elevation of the SRTM model was globally adjusted via the Data Calculator tool (GMS), and the flow budget (ET flow out) in May (when evaporation at P2 is maximum) was evaluated. The results are shown in Table 10.

The data show that the relationship between the two is consistent with existing research results (He et al., 2024): The unsaturated zone thickness and evaporation are nonlinearly negatively correlated. When the thickness increases from 6.5 m to 9.1 m (consistent with the overestimation in the borehole model), the evaporation decreases sharply by 93% (from 93.92 m^3/d to 6.34 m^3/d). This means that the overestimation of thickness in the borehole model will significantly underestimate groundwater evaporation, thus distorting the groundwater balance calculation.

It should be noted that the non-zero ET flow out (6.34 m^3/d) at an unsaturated zone thickness of 9.1 m (exceeding the preset 4 m extinction depth) seems to contradict the theoretical assumption of "no evaporation beyond 4 m". However, this phenomenon essentially reflects the inherent "parameter combination effect" in groundwater numerical simulations (Konikow and Bredehoeft, 1992). The evaporation simulation here is not determined by extinction depth alone, but jointly regulated by multiple parameters. For example, the relatively high comprehensive hydraulic conductivity (corresponding to the fine sand lithology in the SRTM model, see Section 4.3) enhances the upward migration of deep soil water, while the

Table 10 Variation of ET flow out with unsaturated zone thickness

Type	Values				
Unsaturated zone thickness (m)	6.5	8	9	9.1	10
ET Flow Out (m^3/d)	93.92	30.68	7.14	6.34	0

appropriate specific yield shortens the water migration path—these parameter interactions offset the theoretical restriction of the 4 m extinction depth, resulting in non-zero evaporation at thicknesses greater than 4 m. This verifies the core viewpoint of Konikow and Bredehoeft (1992): Groundwater model results are the product of multi-parameter interaction, rather than the direct reflection of a single theoretical assumption.

4.4 The influence mechanism of surface elevation on the lithology configuration of unsaturated zone

In addition to unsaturated zone thickness, surface elevation errors also affect the lithology configuration of the unsaturated zone, thereby changing the hydrogeological parameters and further affecting the simulation results.

By distorting the spatial form of the stratigraphic interface, surface elevation error leads to errors in the vertical distribution of lithology in the unsaturated zone. In the area of maximum deviation (around G9 in the northeast), a profile is generated along the groundwater flow direction (Fig. 17), revealing the following patterns:

According to the existing water level data combined with simulated water level data analysis, fine sand exposed at the surface is distributed in the unsaturated zone when the water level is low. Combined with parameter partition III and Fig. 17, Table 11 is obtained.

From the above analysis, elevation error causes an increase in the unsaturated zone thickness of the borehole elevation model. This not only changes the lithology composition of the unsaturated zone (adding silt), but also reduces the hydraulic conductivity by 29% (from 7.64 m/d to 5.45 m/d)—this parameter change further weakens vertical infiltration, eventually resulting in water level simulation deviation in the borehole model, forming a progressive effect of "surface elevation error, unsaturated zone lithology deviation, hydrogeological parameter alteration, and water level simulation deviation".

5 Conclusions and suggestions

Using GMS software, this study systematically reveals the key influence mechanism of surface elevation data accuracy on groundwater simulation by comparing groundwater flow models of Zhaozhou County constructed using SRTM DEM and borehole-interpolation elevations, clarifying the application advantages of SRTM DEM in regional groundwater modeling with sparse boreholes, and expanding the research scope of structural uncertainty in groundwater numerical simulation. The main conclusions are as follows:

(1) This study demonstrates that in regions with gentle terrain but microgeomorphic features, SRTM DEM 90M is more suitable for satisfying the topographic foundation requirements of regional groundwater simulation, compared to the

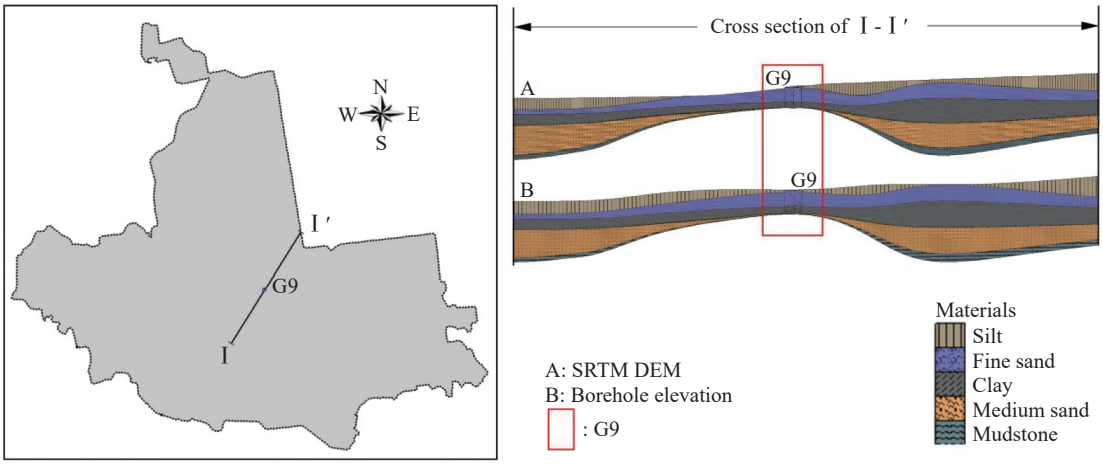


Fig. 17 Lithology configuration difference

Table 11 Comparison of lithology-hydraulic parameters of G9 unsaturated zone

Type	SRTM DEM model	Borehole elevation model
Lithology of unsaturated zone	Fine sand	Silt, fine sand
Hydraulic conductivity (m/d)	7.64	5.45

interpolation of actual boreholes and virtual boreholes.

(2) The over-smoothed terrain induced by borehole interpolation is the core cause of deviations in unsaturated zone thickness and lithology configuration. This deviation continuously impairs the reliability of groundwater simulation results via the progressive pathway of "surface elevation error, unsaturated zone lithology deviation, hydrogeological parameter alteration, and hydrological processes". Even if the water level dynamic fitting meets the required standards, the simulated hydrological processes will be unreliable if there are systematic deviations in the unsaturated zone thickness and lithology configuration. Therefore, model calibration should not only focus on water level fitting, but also incorporate a rationality assessment of the spatial structure of the unsaturated zone.

(3) This study verifies the dominant role of the "parameter combination effect" in simulation. Simulation results are essentially the integrated product of multi-parameter interaction. This highlights that the synergistic influence between parameters should be emphasized during model calibration.

The limitations of this study are that the study area is situated in a plain region (Zhaozhou County) with relatively gentle terrain, so its conclusions should be applied cautiously when extended to mountainous areas with dramatic topographic relief. It is recommended that future research explore the impacts of DEMs with different resolutions on model performance, especially under complex topographic conditions, so as to establish more universal criteria for model top boundary construction.

Acknowledgements

This study was supported by the Basic Research Expenses of Provincial Colleges and Universities of Heilongjiang Province (Project No.: 2022-KYYWF-1238). We thank the Basic Research Expenses of Provincial Colleges and Universities of Heilongjiang Province for their financial support. We also thank Dr. Zhijun Li for providing the necessary raw data for our modelling.

References

Al-Areedhi HH. 2019. Modelling of groundwater flow for the Iraqi Aquifers. Ph. D. Thesis, Iraq: University of Technology.

Beven K. 1989. Changing ideas in hydrology — The case of physically-based models. Journal of Hydrology, 105(1-2): 157−172. DOI：10.1016/0022-1694(89)90101-7.

Baalousha HM. 2012. Modelling surface-groundwater interaction in the Ruataniwha basin, Hawke's Bay, New Zealand. Environmental Earth Sciences, 66: 285−294. DOI：10.1007/s12665-011-1238-y.

Borgia A, Cattaneo L, Marconi D, et al. 2011. Using a MODFLOW grid, generated with GMS, to solve a transport problem with TOUGH2 in complex geological environments: The intertidal deposits of the Venetian Lagoon. Computers & Geosciences, 37(6): 783−790. DOI：10.1016/j.cageo.2010.11.007.

Chen Z, Huang JT, Zhan HB, et al. 2022. Optimization schemes for deep foundation pit dewatering under complicated hydrogeological conditions using MODFLOW-USG. Engineering Geology, 303: 106653. DOI：10.1016/j.enggeo.2022.106653.

Chepkemoi A, Home PG, Raude JM, et al. 2023. Modeling of groundwater potential in Kericho County, Kenya, using GMS_MODFLOW. Scientific African, 19: e01492. DOI：10.1016/j.sciaf.2022.e01492.

Cromwell G, Sweetkind DS, Densmore JN, et al. 2022. Hydrogeologic characterization of the San Antonio Creek Valley watershed, Santa Barbara County, California. Scientific Investigations Report 2022-5001, Groundwater Availability and Use Assessments. US Geological Survey. DOI：10.3133/sir20225001.

Enemark T, Madsen RB, Sonnenborg TO, et al. 2024. Incorporating interpretation uncertainties from deterministic 3D hydrostratigraphic models in groundwater models. Hydrology and Earth System Sciences, 28: 505−523. DOI：10.5194/hess-28-505-2024.

Gaaloul N. 2008. Integrated management of the ground water resources a case study in the Cap-Bon plain in Tunisia. La Houille Blanche, 94(5): 38−44. DOI：10.1051/lhb:2008052.

Gao YH, Shen JH, Chen L, et al. 2023. Influence of underground space development mode on the groundwater flow field in Xiong'an new

area. Journal of Groundwater Science and Engineering, 11: 68−80. DOI：10.26599/jgse.2023.9280007.

He YJ, Wang YY, Liu Y, et al. 2024. Focus on the nonlinear infiltration process in deep vadose zone. Earth-Science Reviews, 252: 104719. DOI：10.1016/j.earscirev.2024.104719.

Hunt RJ, Doherty J, Tonkin MJ. 2007. Are models too simple? Arguments for increased parameterization. Ground water, 45(3): 254−262. DOI：10.1111/j.1745-6584.2007.00316.x.

Harbaugh AW. 2005. MODFLOW-2005: The U. S. Geological Survey modular ground-water model--the ground-water flow process. Techniques and Methods 6-A16. DOI：10.3133/tm6A16.

Høyer AS, Jørgensen F, Sandersen PBE, et al. 2015. 3D geological modelling of a complex buried-valley network delineated from borehole and AEM data. Journal of Applied Geophysics, 122: 94−102. DOI：10.1016/j.jappgeo.2015.09.004.

Konikow LF, Bredehoeft JD. 1992. Ground-water models cannot be validated. Advances in Water Resources, 15: 75−83. DOI：10.1016/0309-1708(92)90033-X.

Kawo NS, Korus J, Gulbrandsen ML. 2023. Multiple-point statistical modeling of three-dimensional glacial aquifer heterogeneity for improved groundwater management. Hydrogeology Journal, 31: 1525−1546. DOI：10.1007/s10040-023-02658-x.

Kheirandish M, Rahimi H, Kamaliardakani M, et al. 2020. Obtaining the effect of sewage network on groundwater quality using MT3DMS code: Case study on Bojnourd plain. Groundwater for Sustainable Development, 11: 100439. DOI：10.1016/j.gsd.2020.100439.

Korus JT, Joeckel RM. 2022. Sandstone-body geometry and hydrostratigraphy of the northern High Plains Aquifer system, USA. Quarterly Journal of Engineering Geology and Hydrogeology, 55: 18. DOI：10.1144/qjegh2021-171.

Langevin CD, Provost AM, Panday S, et al. 2022. Documentation for the MODFLOW 6 Groundwater Transport Model. DOI：10.3133/tm6A61.

Li ZX, Xiao J, Wan JW, et al. 2024. A dynamic modeling approach to predict water inflow during tunnel excavation in relatively uniform rock masses. Tunnelling and Underground Space Technology, 146: 105568. DOI：10.1016/j.tust.2024.105668.

Lyazidi R, Hessane MA, Moutei JF, et al. 2020. Developing a methodology for estimating the groundwater levels of coastal aquifers in the Gareb-Bourag plains, Morocco embedding the visual MODFLOW techniques in groundwater modeling system. Groundwater for Sustainable Development, 11: 100471. DOI：10.1016/j.gsd.2020.100471.

Mcdonald MG, Harbaugh AW. 1988. A modular three-dimensional finite difference groundwater flow model.

Niswonger RG, Allander KK, Jeton AE. 2014. Collaborative modelling and integrated decision support system analysis of a developed terminal lake basin. Journal of Hydrology, 517: 521−537. DOI：10.1016/j.jhydrol.2014.05.043.

Panday S, Langevin CD, Niswonger RG, et al. 2013. MODFLOW–USG version 1: An unstructured grid version of MODFLOW for simulating groundwater flow and tightly coupled processes using a control volume finite-difference formulation.Techniques and Methods 6-A45. DOI：10.3133/tm6A45.

Qiu SW, Liang XJ, Xiao CL, et al. 2015. Numerical simulation of groundwater flow in a river valley basin in Jilin Urban Area, China. Water, 7: 5768−5787. DOI：10.3390/w7105768.

Sahu SK, Jhariya DC. 2023. 3D-Mathematical model to simulate groundwater flow and sulfate concentration in Tantaria watershed, Bemetara district, Chhattisgarh, India. Environment Development and Sustainability, 25: 1667−1683. DOI：10.1007/s10668-022-02115-x.

Wellmann F, Caumon G. 2018. 3-D Structural geological models: Concepts, methods, and uncertainties. In: SCHMELZBACH, C. (ed.) Advances in Geophysics, 59. San Diego: Elsevier Academic Press Inc.

Woolfenden LR, Engott JA, Larsen J, et al. 2022. Simulation of groundwater and surface-water resources of the San Antonio Creek Valley watershed, Santa Barbara County, California. US Geological Survey. DOI：10.3133/

sir20215139.

Yang FR, Lee CH, Kung WJ, et al. 2009. The impact of tunneling construction on the hydrogeological environment of "Tseng-Wen Reservoir Transbasin Diversion Project" in Taiwan. Engineering Geology, 103: 39−58. DOI：10.1016/j.enggeo.2008.07.012.

Zangeneh M, Tabrizi MS, Khosrojerdi A, et al. 2023. Developing a decision-making model for improving the groundwater balance to control land subsidence. Soil and Water Research, 18: 55−65. DOI：10.17221/57/2022-swr.

Zhai HT, Wang JC, Lu YC, et al. 2023. Prediction of the mine water inflow of coal-bearing rock series based on well group pumping. Water, 15(20): 3680. DOI：10.3390/w15203680.

Zhang Q, Yang QK, Cheng J, et al. 2018. Characteristics of 3" SRTM Errors in China. Geomatics and Information Science of Wuhan University, 43(05): 684−690. (in Chinese) DOI：10.13203/j.whugis20160347.